**Article**

# Generation of ribonuclease H2 A subunit (RH2A)-knockout HEK293 cells and analysis of the ribonucleotide content of their genomic DNA

Haruna Yano, So Nishimoto, Mako Kandabashi, Saori Ogawa, Kyoko Matsumoto, Haruka Hara, Misato Baba, Teisuke Takita, and Kiyoshi Yasukawa*

Division of Food Science and Biotechnology, Graduate School of Agriculture, Kyoto University, Sakyo-ku, Kyoto 606-8502, Japan

**Mammalian ribonuclease (RNase) H2 is a trimeric protein consisting of three subunits (catalytic A and accessory B and C). RNase H2 is involved in the removal of misincorporated ribonucleotides from genomic DNA and RNA strands from RNA/DNA hybrids. In humans, mutations in RNase H2 gene have been linked to a severe neuroinflammatory disorder, Aicardi-Goutières syndrome (AGS). Here, we constructed RNase H2 A subunit (RH2A) knockout human embryonic kidney 293 (HEK293) cells. Knockout cells lacked the RNase H2 activity. However, unlike our previous results with mouse fibroblast NIH3T3 cells, the knockout HEK293 cells did not exhibit an accumulation of ribonucleotides in genomic DNA. These results suggest that the effects of knockout of RNase H2 on accumulation of ribonucleotides differ depending on cell species.**

## Introduction

Ribonuclease H (RNase H) [EC 3.1.26.4] degrades RNA strand of RNA/DNA hybrids by specifically hydrolyzing the 5'-phosphodiester bonds of the RNA in a sequence-nonspecific manner. RNase H is classified into types 1 and 2. For activity, type 1 requires at least four consecutive ribonucleotides, while type 2 requires only single ribonucleotide [1−3]. RNase H3 belongs to type 2 but has type 1-like activity. Eukaryotic type 2 RNase H (RNase H2) is a complex containing three protein units, catalytic A subunit and accessory B and C subunits [4–7]. The misincorporation of ribonucleotides into genomic DNA by replicative DNA polymerases leads to genomic instability, causing endogenous DNA damage such as double strand break. RNase H2 removes such ribonucleotides by working together with flap endonuclease (FEN-1), DNA polymerase δ, and DNA ligase 1 [4, 7]; this is called the ribonucleotide excision repair (RER) mechanism [4, 7].

In mammals, RNase H2 plays an essential physiological role at both individual and cellular levels. In humans, mutations of Rnaseh2A, 2B, or 2C cause a severe neuroinflammatory disorder, Aicardi-Goutières syndrome (AGS) [8, 9] and systemic lupus erythematosus (SLE) [10]. In

*Correspondence author: Kiyoshi Yasukawa.
Phone: +81-75-753-6266
E-mail: yasukawa.kiyoshi.7v@kyoto-u.ac.jp

mice, knockout of Rnaseh2A, 2B, or 2C causes embryonic death [11–13]. In cells derived from patients with AGS [14] and RNase H2 A subunit (RH2A) knockout (KO) mice [11], micronuclei accumulated in the cytoplasm, cyclic GMP-AMP synthase (cGAS)/stimulator of interferon genes (STING) pathway was activated, interferon-stimulated genes (ISGs) mRNA expression was elevated, and the amount of ribonucleotide in genomic DNA increased. These events are known as AGS-related cellular events. In human cervical cancer HeLa cells, depletion of RNase H2 induced accumulation of ribonucleotides in the genomic DNA [14]. In mouse embryonic fibroblasts (MEFs) isolated from tamoxifen-inducible RNase H2 KO mice, induced KO of Rnaseh2A exhibited AGS-related events [15]. We reported that RH2A-KO mouse fibroblast NIH3T3 cells exhibited an accumulation of ribonucleotides in genomic DNA, although they did not exhibit elevated ISGs expression [16]. Together with other previous reports [17–20], our results suggested that the accumulation of ribonucleotides in genomic DNA is closely related to the absence of RNase H2, but the degree of subsequent cellular events depend on various factors other than RNase H2,

To explore the molecular mechanism of RNase H2 in AGS, the activity and stability of 36 RNase H2 variants with AGS-causing mutation (18 variants for A, 10 variants for B, and 8 variants for C subunit) were reported [9, 21–23]. Reports show that the activities of A-G37S (Gly37 in the A subunit is replaced with Ser), A-A178V, A-186W, and A-R235Q were less than 1% of that of the wild-type enzyme (WT), whereas those of the other variants were 10–120%. As for stability, the melting temperature ($T_m$) of the CD- or fluorescence-based assay of B-F95L was lower than that of WT by 9°C, whereas those of other variants were equal to or lower by

0.1–3.3°C than WT.

Based on these results, A-G37S was used as a representative variant with markedly low activity. This residue is located close to the active site. We recently reported that when a mouse RH2A variant with a mutation corresponding to the AGS-causing mutation A-G37S was transiently expressed in RH2A-KO NIH3T3 cells, RNase H2 activity in the cellular extract did not increase and ribonucleotide amount in genomic DNA did not decrease. However, when a mouse RH2A variant with a mutation corresponding to another AGS-causing mutation A-N213I or A-R293H, RNase H2 activity increased and ribonucleotide amount decreased [24]. These results suggested that the AGS-causing mechanism of the A-G37S mutation might be ascribed to a decrease in activity, whereas those of other mutations, including A-N213I and A-R293H, remain unknown. In this study, to explore whether these findings also apply to other cells, we constructed human embryonic kidney 293 (HEK293) RH2A-KO cells and characterized them.

**Materials and Methods**

*Construction of plasmid*　For the construction of Cas9-sgRNA expression plasmid, pGuide-it-ZsGreen1-hRNaseH2A, the annealing reaction was carried out in 10 μL of 1 μM oligo-1, 1 μM oligo-2 (Table 1), and 80% v/v Guide-it oligo annealing buffer (Takara Bio, Kusatsu, Japan) at 95°C for 2 min followed by room temperature for 10 min and 4°C for 30 min. The ligation reaction was carried out in 5 μL of 1.5 μg/μL linearized pGuide-it plasmid (Takara Bio), 10 nM annealing products, and 50% v/v DNA Ligation Mighty Mix (Takara Bio) at 16°C for 30 min followed by the transfection into Stellar™ Competent Cells (Takara Bio).

For the construction of human RH2A

expression plasmid, pCMV-hRNaseH2AWT, the DNA fragment corresponding to the vector sequence of pCMV-S_FLAG was amplified by PCR from pCMV-mRNaseH2A [24] using primers pCMV_for2 and pCMV_rev2 (Table 1) and recombinant KOD-Plus-Neo (Toyobo, Osaka, Japan) under 35 cycles at 98ºC for 10 s and 68ºC for 5 min. The DNA fragment encoding human RH2A was from pCMV-hRNaseH2A using primers phRH2Afor2 and phRH2Arev2 (Table 1) under 35 cycles at 98ºC for 10 s and 68ºC for 1 min. These two amplified two fragments were ligated using In-Fusion HD Cloning Kit (Takara Bio), to give pCMV-hRNaseH2A.

Table 1. Oligonucleotide.

| Primers | Sequences (5'-3') |
| --- | --- |
| oligo-1 | CCGGGGAGGCGCCGGCTCCACGCT |
| oligo-2 | AAACAGCGTGGAGCCGGCGCCTCC |
| pCMV_for2 | CTAGAGGCCCTATTCTATAGTG |
| pCMV_rev2 | CGGCCGCGTTATCGTCATCG |
| phRH2Afor2 | GACGATAAGGCGGCCGCTAT GGATCTCAGCGAGCT |
| phRH2Arev2 | GAATAGGGCCTCTAGACTAGA GGGCTGGTTGCTGA |
| primer F | CAGGGATGAATGGCAACTTT |
| primer R | GTGTACTATGTCGGTGACCC |
| primer 1 | GTTCTTGCAGCTGGTGGTGG |
| primer 2 | ATTTGACCCTGTGGTGGGGA |
| primer 3 | TGCATTCATTTATGTTTCAGG |
| primer 4 | TTGTGATGCTCGTCAGGGGG |

*Construction of RH2A-KO cells using CRISPR Cas9 method*   HEK293 cells (Cell Resource Center for Biomedical Research, Institute of Development, Aging and Cancer, Tohoku University) were cultured in 500 μL RPMI 1640 medium containing 10% fetal bovine serum, penicillin, streptomycin and L-glutamine to 50–60% confluency in 12-well microplates with 5% $CO_2$ incubator in a humidified atmosphere at 37ºC. pGuide-it-ZsGreen1-hRNaseH2A (2.5 μg) was transfected using Xfect Transfection Reagent (Clontech, Mountain View, CA). The cells were cultured for 2 days to 100% confluency and cloned by limiting dilution in 96-well microplates.

After 1 month, colonies originating from single cells were transferred to 12-well microplates for expansion. Genomic DNA was prepared from the non-transfected and transfected HEK293 cells using GenElute™ Mammalian Genomic DNA Miniprep Kits (Sigma, St. Louis, MO). The 517-bp fragment was amplified by PCR using primer F and primer R and recombinant KOD-Plus-Neo under 30 cycles of 45 s at 95°C, 30 s at 68°C. The *Nco*I digestion of the PCR products was performed with 1 U *Nco*I at 37°C for 1 h. The products were applied to 2.0% w/v agarose gel and the gel was stained with ethidium bromide (1 μg/mL).

*Construction of RH2A-KO cells using VIKING method*   Plasmid construction and transfection were carried out by Setsuro Tech Inc. (Tokyo Japan) as described previously [25, 27]. Transfected cells were cultured in the presence of 1 μg/mL puromycin and cloned by limiting dilution in 96-well microplates. After 1–3 weeks, colonies originating from single cells were transferred to 12-well microplates for expansion. Genomic DNA was prepared from the non-transfected and transfected HEK293 cells. The 291- and 828-bp fragments were amplified by PCR using primers 1 and 4 and primers 2 and 3 respectively (Table 1) and recombinant KOD-Plus-Neo under 30 s at 95°C followed by 34 cycles of 10 s at 95°C, 30 s at 58 °C, and 30 s at 68°C. The products were applied to 2.0% w/v agarose gel and the gel was stained with ethidium bromide (1 μg/mL).

*Expression of RH2A in RH2A-KO cells* HEK293 cells were cultured to 50–60% confluency in 500 μL of RPMI 1640 medium. pCMV-hRNaseH2AWT, pCMV-

hRNaseH2AG37S, pCMV-hRNaseH2AN212I, or pCMV-hRNaseH2AR291H (each 2.5 μg) was transfected into HEK293 cell, using Xfect Transfection Reagent.

*MTT assay*    MTT assay was performed using MTT Cell Count Kit (Nacalai Tesque, Kyoto, Japan) as described previously [16]. Briefly, 3-(4,5-dimethylthiazol-2-yl)-2,5-diphenyl tetrazolium bromide (MTT) solution and color development solution were added to the HEK293 cells cultured in 96-well microplates ($5 \times 10^3$ cells/mL, 100 μL/well) at indicated time points. The absorbance at 570 nm was measured with EnSight (PerkinElmer, Waltham, MA) with the reference of 650 nm.

*Preparation of cell extract*    Cells ($5 \times 10^7$ cells) were washed with PBS (-) two times and suspended with 1 mL of 50 mM Tris-HCl (pH 8.0) buffer containing 60 mM KCl, 0.1% v/v Triton X-100, 100-fold diluted Protease Inhibitor Cocktail (Nacalai Tesque) followed by sonication. After centrifugation at $15,000 \times g$ at 4°C for 20 min, the supernatant was collected. Protein concentration was determined by the bicinchoninic acid (BCA) method using Protein Assay Bicinchoninate kit (Nacalai Tesque) with bovine serum albumin (Nacalai Tesque) as a standard.

*Western blot*    Twenty μL of the cell extract was mixed with 4 μL of the SDS-PAGE sample buffer (0.25 M Tris-HCl buffer (pH 6.8), 50% v/v glycerol, 10% w/v SDS, 0.6 M dithiothreitol 5% v/v 2-mercaptoethanol, 0.05% w/v bromophenol blue**)** and was boiled for 10 min. The solution (20 μL) was applied to 12.5% w/v SDS-polyacrylamide gel and was run at 40 mA for 40 min. Pre-stained Protein Markers (Nacalai Tesque) consisting of β-galactosidase (112 kDa), bovine serum albumin (87 kDa), glutamine dehydrogenase (59 kDa), ovalbumin (47 kDa), carbonic anhydrase (33 kDa), myoglobin (27

kDa), and lysozyme (20 kDa) was used for marker proteins. After separation, the proteins were transferred by electroblotting onto a polyvinylidene difluoride (PVDF) membrane Sequi- Blot™ PVDF (BioRad, Hercules, CA) in 25 mM Tris-HCl buffer (pH 8.3), 192 mM glycine, 20% v/v methanol at 25 V for 50 min. After blotting, the membrane was washed with 50 mM Tris-HCl buffer (pH 8.3), 138 mM NaCl, 2.7 mM KCl, 0.05% Tween 20 (TBS-T), blocked with TBS-T containing 2% w/v skim milk, and incubated with mouse anti human RH2A polyclonal antibody, Anti RNASEH2A (Proteintech, Rosemont, IL, 1:1000 in TBS-T containing 1% w/v skim milk). Then, the membrane was incubated with HRP-conjugated goat anti-rabbit immunoglobulins (Agilent Technologies, Santa Clara, CA, 1:1000 in TBS-T containing 1% w/v skim milk). After washing with TBS-T for three times, the protein bands were visualized using a Peroxidase Stain Kit (Nacalai Tesque).

*RNase H2 activity assay*    RNase H2 activity assay was performed as described previously [24]. Briefly, 5′-terminus of $DNA_5$-$RNA_1$-$DNA_6$ (5′-GACACcTGATTC-3′) (named 1R) was labeled using [γ-$^{32}$P]ATP (370 MBq/ml; 111 Bq/pmol) (PerkinElmer). Then, a hybrid consisting of the 5'-[$^{32}$P]-labelled 1R and unlabeled complementary DNA (named 1R/12D) was prepared.    The reaction (10 μL) was carried out with indicated concentrations of the cell extracts and 200 nM 1R/12D in 50 mM Tris–HCl buffer (pH 8.0) containing 60 mM KCl and 5 mM $MgCl_2$ at 25ºC for indicated time. The reaction was stopped and analyzed and applied to denaturing 20% polyacrylamide gel and was run. After the electrophoresis, the gel was analyzed by a Typhoon FLA 9500 (GE Healthcare, Buckinghamshire, UK) using the program ImageQuant TL (GE Healthcare). Recombinant

human RNase H2, expressed in *Escherichia coli* and purified from the cells [23, 25, 26], was used as a positive control.

*Alkaline hydrolysis and electrophoresis of genomic DNA*　The procedure was according to our previous report [24]. Briefly, genomic DNA was prepared from the cells using GenElute™ Mammalian Genomic DNA Miniprep Kits (Sigma). The alkaline hydrolysis reaction was carried out in 26 μL of 0.23 μg/μL genomic DNA, 0.23 M KOH at 55ºC for 2 h. After adding alkaline sample-loading buffer (4 μL of 300 mM KOH, 6 mM EDTA, pH 8.0, 18 % glycerol, 0.15 % bromocresol green, 0.25 % xylene cyanol FF), the solution (30 μL) was applied to 1% w/v alkaline agarose gel in 50 mM NaOH, 1 mM EDTA and was run at 20 V for 13 h. After neutralization with 1 M Tris-HCl buffer (pH 7.6) containing 1.5 M NaCl for 3 h, the gel was stained with SYBR Gold (Thermo Fisher Scientific, Waltham, MA) diluted 10,000-fold with 1 × TAE.

## Results

### Establishment of RH2A-KO HEK293 cells by CRISPR/Cas9

We analyzed the nucleotide sequence of the subunit A (accession number NM_006397.3) using CRISPRdirect (https://crispr.dbcls.jp/), and selected exon 1 (67 bp) of RH2A gene as a target sequence where Cas9 cleaves double-stranded DNA. The exon 1 has CCCATGG comprising the PAM sequence (CCC) and the *Nco*I recognition site (CCATGG) at the 5' terminus (Fig. 1A). Figure 1B shows the sequence of the 517-bp fragment containing the entire exon 1 amplified by PCR from the genomic DNA of the wild-type HEK293 (WT) cells. It has the *Nco*I recognition site at the position 68. Figure 1C shows pGuide-it-ZsGreen1-hRNaseH2A, which we constructed

as the expression plasmid of sgRNA and Cas9. The 517-bp fragment containing the entire exon 1 was amplified from the genomic DNA of WT or each clone.



**Fig. 1.** Knockout of *Rnaseh2a* gene of HEK293 cells with the CRISPR/Cas9 system.

(A) Target site in the *Rnaseh2a* gene coding the RNase H2 A subunit. (B) Nucleotide sequence of the PCR product amplified from the genomic DNA of the wild-type HEK293 (WT) cells with a primer combination of primer F and primer R. The PAM and target sequences are indicated by a box with solid and dashed lines, respectively. The *Nco*I recognition site, primer binding sites and nucleotide sequences of the exon 1 are indicated by solid, dashed, and double underlines, respectively. The solid arrow indicates the Cas9 cleavage site. (C) Plasmid for the expression of sgRNA and Cas9. The PAM and target sequences are indicated by a box with solid and dashed lines, respectively.

Figure 2A shows the agarose gel electrophoresis of the *Nco*I-untreated or treated fragments. In the WT and clones 1, 3, 5, 6 8, and 9, 450 bp-band was detected, which was thought to be the fragment resulted from the cleavage by *Nco*I. In clone 7, only 517 bp-band was detected, suggesting that it was homo *Nco*I site-deleted clones. Figure 2B shows the sequence of clone 7 near the cleavage site. Two overlapping profiles were observed, showing that deletion occurred at different sites in two *Rnaseh2a* genes. We selected clone 7 for the subsequent analysis.
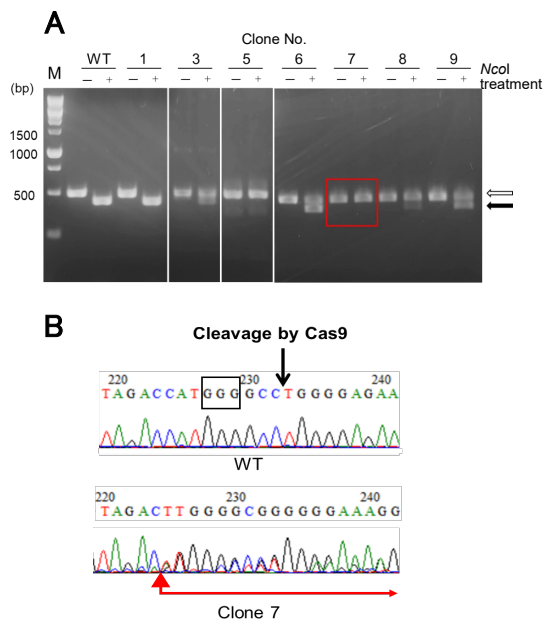


**Fig. 2.** Screening of *Rnaseh2a-/-* homozygote HEK293 cells.
(A) Patterns of agarose gel electrophoresis. PCR products amplified from the genomic DNA of the WT and clones 1, 3, and 5–9 cells were digested with *Nco*I and applied to 2% w/v agarose gel. The arrow indicates the 517-bp band corresponding to the PCR product which was not cleaved by *Nco*I. The solid arrow indicates the 451-bp band corresponding to the PCR product which was cleaved. (B) Nucleotide sequences of the exon 1 of the Rnaseh2a gene in the WT and clone 7 (KO) cells. The solid underline in WT indicates the sequence which was deleted in clone 4, and the red arrow triangle in Clone 7 indicates the site at which the deletion occurred. The PAM sequence is indicated by a box.

## Microscopic image and growth curve of HEK293 cells

In microscopic analysis (Fig. 3A), there is no difference in size and shape between HEK293 wild-type (WT) and RH2A-KO cells. In MTT assay (Fig. 3B), the absorbance at 570 nm ($A_{570}$) of the culture medium to which MTT reagent was added at indicated time points increased with time and reached the highest at day 2.5 in the WT cells and at day 4 in the RH2A-KO cells. This indicated that the growth rate of the RH2A-KO cells was lower than that of the WT cells. The slopes of the line expressing the $\log_2(A_{570})$ values (y) at day x of the WT and RH2A-KO cells were 1.3 and 0.8, suggesting that the growth rate of the RH2A-KO cells was 60% of that of the WT cells.

## Time-course analysis of protein level of RNase H2 in the cellular extract

To examine the effect of transient expression of RNase H2, we constructed the expression plasmid for RH2A (Fig. 4A), which contains the CMV promoter followed by a DNA sequence encoding human RH2A. We transfected it in RH2A-KO HEK293 cells. Western blot analysis was performed to assess the protein existence of RH2A (Fig. 4B). In recombinant N-terminally (His)$_6$-tagged human RNase H2 and WT cells, an about 35 kDa protein band corresponding to RH2A and a 45 kDa band corresponding to β-actin were detected. In RH2A-KO cells, the former was not detected, but the latter was detected, indicating that the RH2A-KO cells did not express RH2A. In the RH2A-KO cells transfected with expression plasmid for N-terminally FLAG-tagged human RH2A, a 40-kDa protein band corresponding to RH2A and a 45-kDa band corresponding to β-actin were detected between days 1–10. The reason for the difference
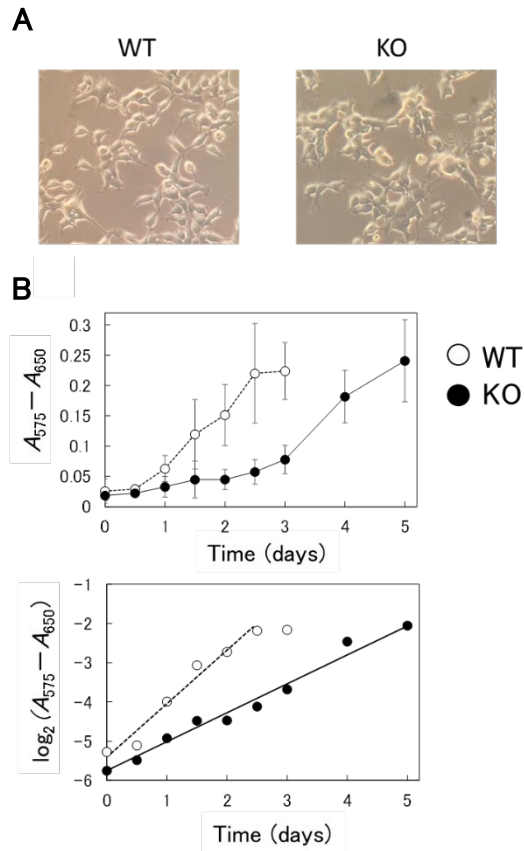
**Fig. 3.** Microscopic image and growth curve of HEK293 WT and RH2A-KO cells.

(A) Microscopic images. WT (left panel) and RH2A-KO (right panel) cells at ×200 magnification are shown. (B) Growth curves. WT (upper panel) and RH2A-KO cells (lower panel) were added to 96-well microplates and cultured. At the time indicated, MTT reduction was measured. Error bars indicate SD values for eight-time measurements. Vertical axis in upper panel is changed to a logarithmic scale in lower panel. In the lower panel, the plot at day 3 was not used to make a line.

in molecular mass between WT cells (35 kDa) and transfected RH2A-KO cells (40 kDa) is unknown. These results indicate that RH2A was expressed in the transfected RH2A-KO cells for 10 days after transfection with the expression plasmid for RH2A. As with our previous study on RH2A-KO NIH3T3 cells [24], RNA/DNA hybrid
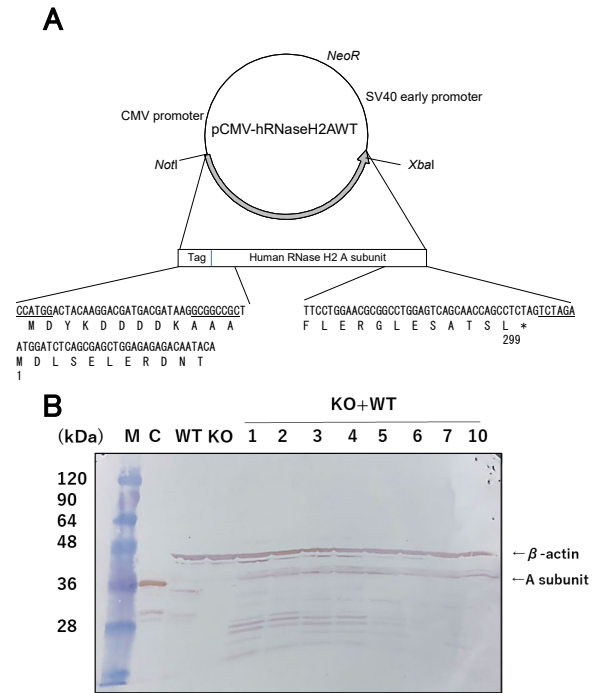


**Fig. 4.** Expression of RH2A.

(A) Expression plasmid for human RH2A. The construction of pCMV-hRNaseH2AWT is shown. The asterisk indicates the termination codon. *Not*I and *Xba*I sites are underlined. The number indicates the amino acid number of RH2A. (B) Western blot analysis. Extracts of WT cells, RH2A-KO cells, or RH2A-KO cells transfected with pCMV-hRNaseH2AWT and cultured for indicated days (1–10 days) were applied to 12.5% w/v SDS-polyacrylamide gel. As a positive control, 340 ng of purified recombinant human RNase H2 was used instead of extracts. After transferring the protein onto a PVDF membrane, the membrane was incubated with anti β-actin antibody or anti-RH2A antibody as a primary antibody and HRP-conjugated rabbit anti-mouse antibody or HRP-conjugated goat anti-rabbit antibody as a secondary antibody. The open and solid arrows indicate the bands corresponding to RH2A and β-actin, respectively.

(1R/12D) consisting of a 5'-[$^{32}$P]-labelled DNA$_5$-RNA$_1$-DNA$_6$ (1R) and an unlabeled complementary DNA (12D) was used as a substrate. This substrate is designed to produce a 5'-[$^{32}$P]-labelled 5-nt DNA when RNase H2 cleaves it.

Figure 5 shows the denatured PAGE analysis

of the products obtained from the reaction under various conditions. In the reaction with recombinant human RNase H2, only the 5-nt band was detected, indicating that recombinant human RNase H2 cleaved 1R/12D completely. The 5-nt band was detected clearly at 1 µg protein amount

**A**



**B**



**Fig. 5.** Expression of RH2A.

RNase H2 activity in the RH2A-KO cells transfected with RNase H2 expression plasmid.

The reaction (7.5 µL) was carried out with 200 nM 1R/12D in the presence of 100 ng, 1 µg, or 10 µg of extracts of WT cells, RH2A-KO cells, or RH2A-KO cells transfected with pCMV-hRNaseH2AWT and then cultured for indicated days (1–10 days), at pH 8.0 at 25°C for 20 min. As a positive control, 8.6 ng of purified recombinant human RNase H2 was used instead of extracts. Then, the reaction solutions were applied to 20% w/v denaturing polyacrylamide gel. The open and solid arrows indicate the bands corresponding to the 12-nt RNA fragment and cleavage products, respectively.

for WT cells whereas it was faintly detected at 10 µg protein amount for RH2A-KO cells, In the reaction with the RH2A-KO cells transfected with expression plasmid for RH2A, the 5-nt band at 10 µg protein amount was stably detected between days 1–10, indicating that KO cells exhibited RNase H2 activity for at least 10 days after transfection of expression plasmid for RH2A.

**Expression of RH2A variant with an AGS-causing mutation**

We analyzed the effects of transient expression of human RH2A variants, G37S, N212I, and R291H (corresponding to mouse G37S N213I and R293H), in the RH2A-KO cells. Figure 6A and B show the RNase H2 activity in the cell extract. The 5-nt band was detected faintly at 1 µg and clearly at 10 µg protein amount for WT cells, whereas it was not detected at 1 µg and faintly detected at 10 µg protein amount for RH2A-KO cells. The RH2A-KO cells transfected with the expression plasmid or G37S exhibited the similar pattern as untransfected RH2A-KO cells, whereas those transfected with the expression plasmid N212I or R291H exhibited the similar pattern as WT cells.

Figure 6C and D show the amounts of ribonucleotides in the genomic DNA. RH2A-KO cells exhibited slightly increased mobility compared to that of the WT cells. Unlike the case with the RNase H2A activity, there were almost no difference in ribonucleotide accumulation among the RH2A-KO cells and the RH2A-KO cells transfected with the expression plasmid for the wild-type RH2A, G37S, N212I or R291H.

**Establishment of RH2A-KO HEK293 cells by VIKING method**

As described above, the RH2A-knockout HEK293 cells established by CRISPR/Cas9 system did not exhibit an accumulation of

## A

Transfected RH2-KO cells



## B



## C

Transfected RH2-KO cells



## D
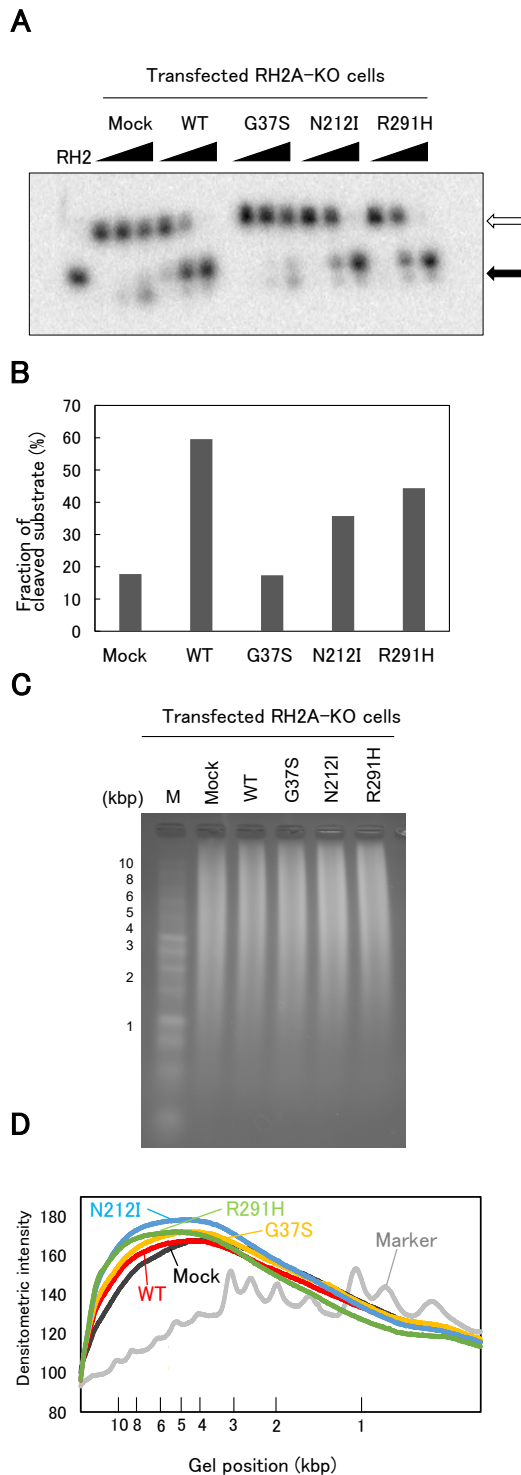


**Fig. 6.** Expression of RH2A variants with AGS-causing mutation in RH2A-KO cells.

RH2A-KO cells were transfected with either pCMV_S-FLAG (Mock), pCMV-hRNaseH2AWT, pCMV-hRNaseH2AG37S, pCMV-hRNaseH2AN212I, or pCMV-hRNaseH2AR291H and then cultured for 2 days. (A, B) RNase H2 activity. The reaction (7.5 µL) was carried out with 200 nM 1R/12D in the presence of 100 ng, 1 µg, or 10 µg of extracts of transfected cells at pH 8.0 at 25ºC for 20 min. As a positive control, 8.6 ng of purified recombinant human RNase H2 was used instead of extracts. Then, the reaction solutions were applied to 20% w/v denaturing polyacrylamide gel. (A) Image scanning. The open and solid arrows indicate the bands corresponding to the 12-nt RNA fragment and cleavage products, respectively. (B) ImageJ analysis of the reaction products in the presence of 10 µg of extracts of the transfected RH2A-KO cells. (C, D) Alkaline agarose gel electrophoresis. Alkaline-treated genomic DNA of the transfected RH2A-KO HEK293 cells was applied to 1% w/v alkaline agarose gel. (C) SYBR Gold-stained gel. (D) Densitometry scanning of the lanes in (C). One of the representative results of triplicate determination is shown.

ribonucleotides in genomic DNA. To further address this issue, we attempted to construct RH2A-knockout HEK293 cells using the VIKING method and characterize them.

As shown in Fig. 7A, we selected three target sequences, Target 1 in exon 1 and Targets 2 and 3 in exon 3. In the VIKING method, the donor vector contains a puromycin resistance gene. After the transfection of the target gene-cleaving vectors containing Target 1, 2 or 3 sequence, the cells were cultured in the presence of puromycin. After the cloning, two clones were obtained from the cells transfected with the vector containing Target 3 sequence. Figure 7B shows the design of PCR used for the screening. In Target 3, the PCR products 1 2, 3, 4, and 5 were designed to be 356, 291, 763, 828, and 786 bp. As shown in Fig. 7C, only PCR products 2, 4, and 5 appeared in Clone 1 while all five PCR products appeared in Clone 2. This suggested that the vectors were inversely inserted in the RH2A genes in Clone 1 while the vectors were positively and inversely inserted in the RH2A gene in Clone 2. Figure 7D shows the results of western blot analysis. In recombinant human RNase H2, WT cells, and Clone 2, a
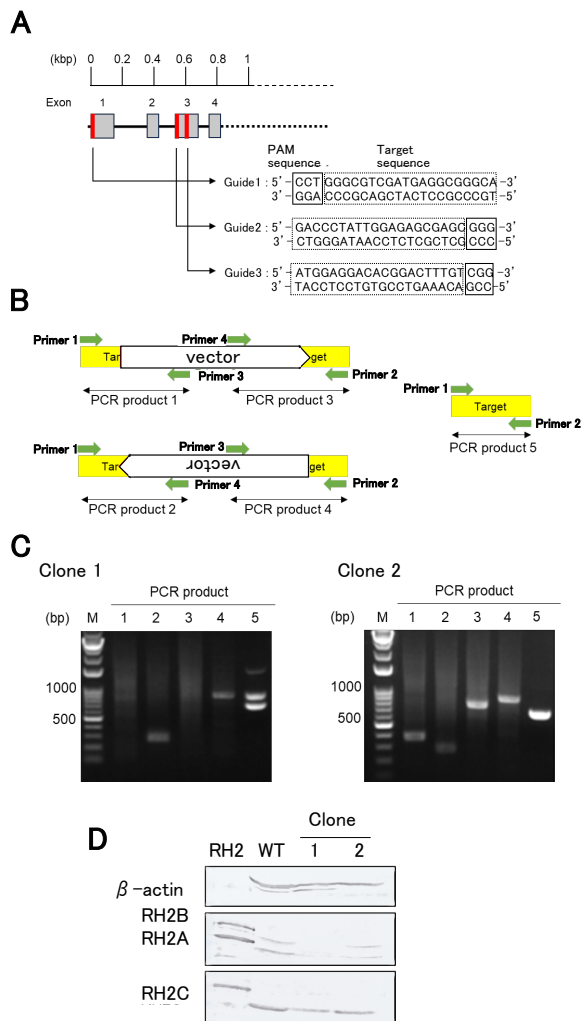
**Fig. 7.** Knockout of *Rnaseh2a* gene of HEK293 cells with the VIKING system.

(A) Design of knockout of *Rnaseh2a* gene of HEK293 cells. Target-site sequences are shown. (B) Target sites of Primers 1–4. (C) Patterns of agarose gel electrophoresis. PCR products amplified from the genomic DNA of Clones 1 and 2 were applied to 2.0% w/v agarose gel. (D) Western blot. Cellular extracts of WT, Clone 1, and Clone 2 cells were applied to 12.5% w/v SDS-polyacrylamide gel. As a positive control, 215 ng of purified recombinant human RNase H2 containing N-terminal (His)$_6$ at each subunit was used instead of extracts (lane RH2). After transferring the protein onto a PVDF membrane, RH2A and β-actin were detected using rabbit anti-RNase H2 polyclonal antiserum and mouse anti-β-actin monoclonal antibodies, respectively.

protein band corresponding to RH2A was detected,

while in Clone 1, it was not detected. This indicated that Clone 1 has an intact RNase H2 gene, suggesting that HEK293 has more than two RH2A genes.

Figure 8A and B show the RNase H2 activity in the cell extract. The 5-nt band was detected faintly at 1 μg and clearly at 10 μg protein amount for WT and Clone 2 cells, whereas it was not detected at 1 μg and faintly detected at 10 μg protein amount for Clone 1 cells. Figure 8C and D show the amounts of ribonucleotides in the genomic DNA. There were almost no difference in ribonucleotide accumulation among the WT, Clone 1, and Clone 2 cells. These results indicated that like the case with the RH2A-KO HEK293 cells established by CRISPR/Cas9 system, the RH2A-KO HEK293 cells established by VIKING method lacked the RNase H2 activity, but did not exhibit an accumulation of ribonucleotide in the genomic DNA.

## Discussion

Decreased RH2 activity was observed in RH2A-KO HEK293 cells (Fig. 5). However, increased ribonucleotide content in genomic DNA was not observed (Fig. 6). In the absence of RH2, topoisomerase is responsible for removing ribonucleotides from the genomic DNA [6, 29]. Our results suggest a possibility that the degree of RH2-independent RER activity is higher in HEK293 cells than in NIH3T3 cells. However, Zimmermann *et al.* reported that topoisomerase increases endogenous DNA double strand break in RNase H2-deficient cells, declining this possibility [30].

RH2A-KO HEK293 cells exhibit the same morphology—but slower growth— than WT HEK293 cells (Fig. 3). These results agreed with our previous results generated using NIH3T3 cells. Pizzi et al. reported that RNA interference-mediated RNase H2 (RH2) depletion impaired
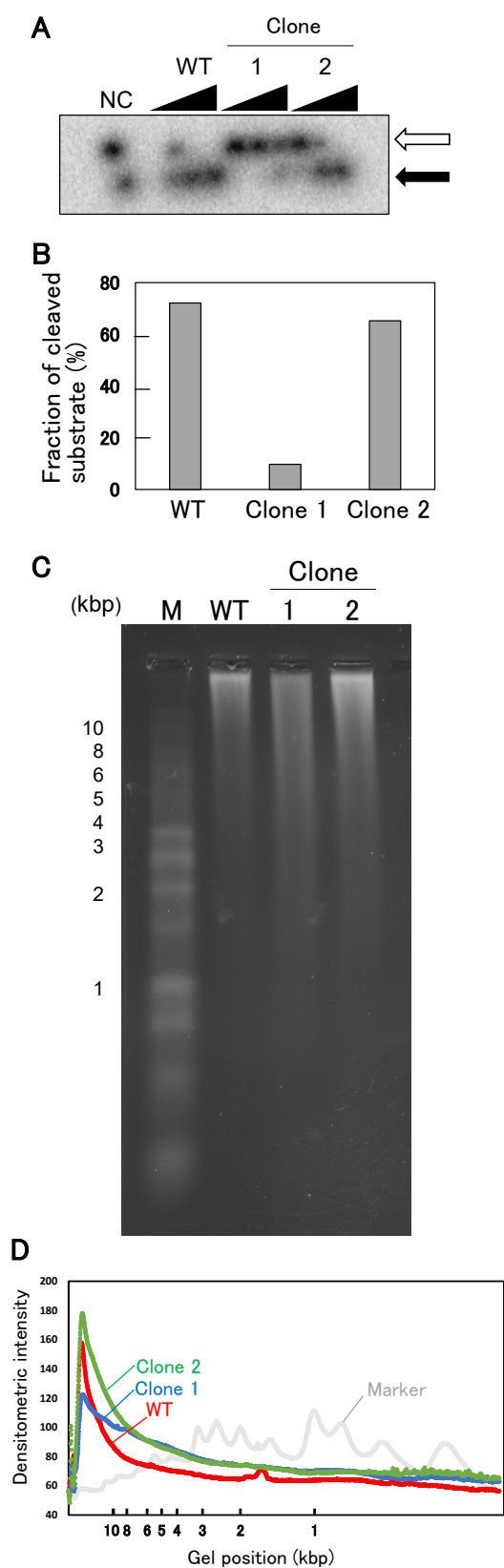
**Fig. 8.** Characterization of RH2A-KO cells.

(A, B) RNase H2 activity. (A) Image scanning. The open and solid arrows indicate the bands corresponding to the 12-nt RNA fragment and cleavage products, respectively. (B) ImageJ analysis of the reaction products in the presence of 10 μg of extracts of the transfected RH2A-KO cells. (C, D) Alkaline agarose gel electrophoresis. Alkaline-treated genomic DNA was applied to 1% w/v alkaline agarose gel. (C) SYBR Gold-stained gel. (D) Densitometry scanning of the lanes in (C). One of the representative results of triplicate determination is shown.

cell growth, a phenomenon that they ascribed to defects in completing the S-phase and to G2/M arrest [14]. We speculate that RH2A knockout would induce similar replication stress in HEK293 and NIH3T3 cells.

When an RH2A variant (G37S) with an AGS-causing mutation was expressed in RH2A-KO HEK293 cells, no increase in RH2 activity in cell extracts was observed (Fig. 6A and B). By contrast, increase in RH2 activity was observed upon expression of N212I and R291H (Fig. 7A and B). This raises the question "how do the N212I and R291H mutations—and probably a number of other AGS-causing mutations that do not appreciably affect activity—cause AGS?". Cristini *et al.* recently used chromatin immunoprecipitation with an anti-RH2 antibody to show that RH2 is recruited to a specific subset of genes in a transcription-dependent manner and that it suppresses the accumulation of R-loops in cells [31]. We speculate that some AGS mutations, including RH2A N212I and R291H variants, cause AGS by impairing the protein-protein interactions required for such cellular events.

In conclusion, RH2A-KO HEK293 cells lacked hydrolytic activity toward single ribonucleotides in duplex DNA and exhibited retarded growth, but not presented higher ribonucleotide content in genomic DNA than WT

43

cells. Our results suggest that decrease in RNase H2 activity does not necessarily lead to accumulation of ribonucleotides.

## References

[1] Cerritelli, S.M., Crouch, R.J. (2009) *FEBS J.* **276**, 1494–1505.

[2] Champoux, J.J., Schultz, S.J. (2009) *FEBS J.* **276**, 1506–1516.

[3] Tadokoro, T., Kanaya, S. (2009) *FEBS J.* **276**, 1482–1493.

[4] Sparks, J.L., Chon, H., Cerritell, S.M, Kunkel, T.A., Johansson, E., Crouch, R.J., Burgers, P.M. (2012) *Mol. Cell* **47**, 980–986.

[5] Williams, J.S., Kunkel, T.A. (2014) *DNA repair* **19**, 27–37.

[6] Cerritelli, S.M., Crouch, R.J. (2016) *Trends Biochem. Sci.* **41**, 434–445.

[7] Rychlik, M.P., Chon, H., Cerritelli, S.M., Klimek, P., Crouch, R.J., Nowotny, M. (2010) *Mol. Cell* **40**, 658–670.

[8] Crow, Y.J., Leitch, A., Hayward, B.E., Garner, A., Parmer, R., Griffith, E., Ali, M., Semple, C., Aicardi, J., Babul-Hirji, R., Baumann, C., Baxter, P., Bertini, E., Chandler, K.E., Chitayat, D., Cau, D., Déry, C., Fazzi, E., Goizet, C., King, M.D., Klepper, J., Lacombe, D., Lanzi, G., Lyall, H., Martínez-Frías, M.L., Mathieu, M., McKeown, C., Monier, A., Oade, Y., Quarrel, O.W., Rittey, C.D., Rogers, R.C., Sanchis, A., Stephenson, J.B., Tacke, U., Till, M., Tolmie, J.L., Tomlin, P., Voit, T., Weschke, B., Woods, C.G., Lebon, P., Bonthron, D.T., Ponting, C.P., and Jackson, A.P. (2006) *Nat. Genet.* **38**, 910–916.

[9] Coffin, S.R., Hollis, T., Perrion, F.W. (2011) *J. Biol. Chem.* **286**, 16984–16991.

[10] Günther, C., Kind, B., Reijns, M.A., Berndt, N., Martinez-Bueno, M., Wolf, C., Tüngler, V., Chara, O., Lee, Y.A., Hübner, N., Bicknell, L., Blum, S., Krug, C., Schmidt, F., Kretschmer, S., Koss, S., Astell, K.R., Ramantani, G., Bauerfeind, A., Morris, D.L., Cunninghame Graham, D.S., Bubeck, D., Leitch, A., Ralston, S.H., Blackburn, E.A., Gahr, M., Witte, T., Vyse, T.J., Melchers, I., Mangold, E., Nöthen, M.M., Aringer, M., Kuhn, A., Lüthke, K., Unger, L., Bley, A., Lorenzi, A., Isaacs, J.D., Alexopoulou, D., Conrad, K., Dahl, A., Roers, A., Alarcon-Riquelme, M.E., Jackson, A.P., Lee-Kirsch, M.A. (2015) *J. Clin. Invest.* **125**, 413–424.

[11] Uehara, R., Cerritelli, S.M., Hasin, N., Sakhuja, K., London, M., Iranzo, J., Chon, H., Grinberg, A., Crouch, R.J. (2018) *Cell Rep.* **25**, 1135–1145.

[12] Reijns, M.A., Rabe, B., Rigby, R.E., Mill, P., Astell, K.R., Lettice, L.A., Boyle, S,. Leitech, A., Keighren, M., Kilanowski, F., Devenney, P.S., Sexton, D., Grimes, G., Holt, I.J., Hill, R.E., Taylor, M.S., Lawson, K.A., Dorin, J.R., Jackson, A.P. (2012) *Cell* **149,** 1008–1022.

[13] Hiller, B., Achleitner, M., Glage, S., Naumann, R., Behrendt, R., Roers, A. (2012) *J. Exp. Med.* **209**, 1419–1426.

[14] Pizzi, S., Sertic, S., Orcesi, S., Cereda, C., Bianchi, M., Jackson, A.P., Lazzaro, F., Plevani, P., Muzi-Falconi, M. (2015) *Hum. Mol. Genet.* **24**, 649–658.

[15] Bartsch, K., Knittler, K., Borowski, C., Rudnik, S., Damme, M., Aden, K., Spehlmann, M.E., Frey, N., Saftig, P., Chalaris, A., Rabe, B. (2017) *Hum. Mol. Genet.* **26**, 3960–3972.

[16] Tsukiashi, M., Baba, M., Kojima, K., Himeda, K., Takita, T., and Yasukawa, K. (2019) *J. Biochem.* **165**, 249–256.

[17] Hiller, B., Achleitner, M., Glage, S., Naumann, R., Behrendt, R., Roers, A. (2012) *J. Exp. Med.* **209**, 1419−1426.

[18] Rabe, B. (2012) *J. Mol. Med.* **91**, 1235−1240.

[19] Kalhorzadeh, P., Hu, Z., Cools, T., Amiard, S., Willing, E.M., De Winne, N., Gevaert, K., De Jaeger, G., Schneeberger, K., White, C.I., De Veylder, L. (2014) *Plant Cell* **26**, 3680−3692.

[20] Cornelio, D.A., Sedam, H.N., Ferrarezi, J.A., Sampaio, N.M., Argueso, J.L. (2017) *DNA Repair* **52**, 110−114.

[21] Chon, H,, Vassilev, A., DePamphilis, M.L., Zhao, Y., Zhang, J., Burgers, P.M., Crouch, R.J., Cerritelli, SM. (2009) *Nucleic Acids Res.* **37**, 96–110.

[22] Aden, K., Bartsch, K., Dahl, J., Reijns, M.A.M., Esser, D., Sheibani-Tezerji, R., Sinha, A., Wottawa, F., Ito, G., Mishra, N., Knittler, K., Burkholder, A., Welz, L., van Es, J., Tran, F., Lipinski, S., Kakavand, N., Boeger, C., Lucius, R., von Schoenfels, W., Schafmayer, C., Lenk, L., Chalaris, A., Clevers, H., Röcken, C., Kaleta, C., Rose-John, S., Schreiber, S., Kunkel, T., Rabe, B., Rosenstiel, P. (2019) *Gastroenterology* **156** 145–159.

[23] Nishimura, T., Baba, M., Ogawa, S., Kojima, K., Takita, T., Crouch, R. J., Yasukawa, K. (2019) *J. Biochem.* **166**, 537–545.

[24] Kandabashi, M., Yano, H., Hara, H., Ogawa, S., Kamoda, K., Ishibashi, S., Himeda, K., Baba, M., Takita, T., Yasukawa, K. (2022) *J. Biochem.* **172**, 225–231.

[25] Hara, H., Yano, H., Akazawa, K., Kamoda, K., Kandabashi, M., Baba, M., Takita, T., Yasukawa, K. (2023) *Biosci. Biotechnol. Biochem.* **87**, 865–876.

[26] Baba, M., Kojima, K., Nakase, R., Imai, S., Yamasaki, T., Takita, T., Crouch, R.J., Yasukawa, K. (2017) *J. Biochem.* **162**, 211–219.

[27] Sawatsubashi, S., Joko, Y., Fukumoto, S., Matsumoto, T., and Sugano, S.S. (2018) *Sci. Rep.* **8**, 593.

[28] Baba, M., Kojima, K., Nishimura, T., Sugiura, T., Takita, T., Uehara, R., Crouch, R. J., Yasukawa, K. (2020) *PLoS One* **15**, e0228774.

[29] Williams, J.S., Kunkel, T.A. （2018） *Methods. Mol. Biol.* **1703**, 241–257.

[30] Zimmermann, M., Murina, O., Reijns, M.A.M., Agathanggelou, A., Challis, R., Tarnauskaitė, Ž., Muir, M., Fluteau, A., Aregger, M., McEwan, A., Yuan, W., Clarke, M., Lambros, M.B., Paneesha, S., Moss, P., Chandrashekhar, M., Angers, S., Moffat, J., Brunton, V.G., Hart, T., de Bono, J., Stankovic, T., Jackson, A.P., Durocher, D. *Nature* **59**, 285–289.

[31] Cristini, A., Tellier, M., Constantinescu, F., Accalai, C., Albulescu, L.O., Heiringhoff, R., Bery, N., Sordet, O., Murphy, S., Gromak, N. (2022) *Nat. Commun.* **13**, 2961.

Communicated by Hisaaki Mihara